Change in the topology of the glass forming liquid $GeSe_2$ with increasing temperature

1999 J. Phys.: Condens. Matter 11 10219

(http://iopscience.iop.org/0953-8984/11/50/314)

J. Phys.: Condens. Matter **11** (1999) 10219–10227. Printed in the UK PII: S0953-8984(99)06854-X

Change in the topology of the glass forming liquid $GeSe_2$ with increasing temperature

Ingrid Petri†, Philip S Salmon† and W Spencer Howells‡

† Department of Physics, University of Bath, Bath BA2 7AY, UK

‡ ISIS Facility, Rutherford Appleton Laboratory, Chilton, Didcot, Oxon OX11 0QX, UK

Received 11 August 1999

Abstract. The change in topology with increasing temperature of liquid $GeSe_2$ was studied by using neutron diffraction to measure the Bhatia–Thornton number–number partial structure factor, $S_{NN}(Q)$, where Q is the scattering vector. As the temperature is raised from 800 to 1100 °C there is a broadening but little other change in the peaks describing the local coordination environment. There is, however, a collapse of the intermediate range atomic ordering of the network associated with the Ge–Ge correlations as manifest by a substantial reduction in the height of the first sharp diffraction peak and a shift in its position from 0.99(1) to 1.05(1) $Å^{-1}$. The changes in the structure with increasing temperature mimic those observed as the composition of liquid $GeSe_2$ is changed to the GeSe stoichiometry by the addition of germanium. The significance of the results for recent Car–Parinello type *ab-initio* molecular dynamics simulations is briefly discussed.

1. Introduction

The object of this paper is to investigate the change in topology with increasing temperature of the liquid semiconductor $GeSe_2$ by using neutron diffraction to measure the Bhatia–Thornton (1970) number–number partial structure factor, $S_{NN}(Q)$, where Q is the magnitude of the scattering vector. The $GeSe_2$ system was chosen for investigation since it is a much-studied proto-typical glass former for which there is evidence in the liquid state of a breakdown in the network structure and an eventual semiconductor–metal transition with increasing temperature (Andreev *et al* 1976). For example, the conductivity gap in the liquid decreases from 1.4 eV at 750 °C to about zero at 1073 °C while the electrical conductivity rises from 0.05 to 100 Ω^{-1} cm^{-1} (Okada *et al* 1996). Accompanying these changes is an *increase* in the mass density with temperature (Ruska and Thurn 1976) and a reduction in the viscosity that is much more rapid than for other Ge–Se liquids (Glazov and Situlina 1969, Laugier *et al* 1977). Another glass forming binary network melt that shows a semiconductor–metal transition with increasing temperature is As_2Se_3 (Hosokawa *et al* 1991, 1992, Tamura *et al* 1992, Shimojo *et al* 1999).

The total structure factors, $S_T(Q)$, for many binary glasses and their corresponding liquids display a characteristic three-peak structure for $0 \leqslant Qr_1 \leqslant 10$ (Wright *et al* 1985), where r_1 is the nearest-neighbour distance, the origin of which can be traced to $S_{NN}(Q)$ (Salmon 1992). Information on the topology of these systems is thereby provided since the corresponding partial pair distribution function $g_{NN}(r)$ describes the sites of the nuclei but does not distinguish between them. The first of these three peaks in $S_T(Q)$, which is a prominent feature in liquid and glassy $GeSe_2$ (see e.g. Susman *et al* 1990, Fischer-Colbrie and Fuoss 1990, Penfold and Salmon 1991, 1992), is the so-called first sharp diffraction peak (FSDP). It is a signature that

0953-8984/99/5010219+09$30.00

the bonding takes a significant directional character and gives information on the intermediate range atomic ordering (Salmon 1992, 1994). The present experiments on $GeSe_2$ will therefore give information on the melt topology at both short and intermediate length scales.

2. Theory

In a neutron diffraction study of a binary Ge–Se compound, the coherent scattered intensity can be represented by the total structure factor

$$S_T(Q) = [S_{NN}(Q) - 1] + A[\{S_{CC}(Q)/c_{Ge}c_{Se}\} - 1] + BS_{NC}(Q) \tag{1}$$

where c_α and b_α denote the atomic fraction and coherent scattering length of chemical species α, $\Delta b = b_{Ge} - b_{Se}$, $\langle b\rangle = (c_{Ge}b_{Ge} + c_{Se}b_{Se})$, $A = c_{Ge}c_{Se}\Delta b^2/\langle b\rangle^2$ and $B = 2\Delta b/\langle b\rangle$. In equation (1) $S_{NN}(Q)$, $S_{CC}(Q)$ and $S_{NC}(Q)$ are the Bhatia–Thornton (1970) number–number, concentration–concentration and number–concentration partial structure factors respectively. The total pair distribution function follows from the Fourier transform relation

$$G_T(r) = \frac{1}{2\pi^2 n_0 r}\int_0^\infty \mathrm{d}Q S_T(Q) Q \sin(Qr) = [g_{NN}(r) - 1] + Ag_{CC}(r) + c_{Ge}c_{Se}Bg_{NC}(r) \tag{2}$$

where n_0 is the atomic number density. In terms of the partial pair distribution functions, $g_{\alpha\beta}(r)$, for the Ge and Se atomic species,

$$g_{NN}(r) = c_{Ge}^2 g_{GeGe}(r) + c_{Se}^2 g_{SeSe}(r) + 2c_{Ge}c_{Se}g_{GeSe}(r) \tag{3a}$$

$$g_{CC}(r) = c_{Ge}c_{Se}[g_{GeGe}(r) + g_{SeSe}(r) - 2g_{GeSe}(r)] \tag{3b}$$

$$g_{NC}(r) = c_{Ge}g_{GeGe}(r) - c_{Se}g_{SeSe}(r) + (c_{Se} - c_{Ge})g_{GeSe}(r) \tag{3c}$$

and the mean number of particles of type β contained in a volume defined by two concentric spheres of radii r_i and r_j, centred on a particle of type α, is given by

$$\bar{n}_\alpha^\beta = 4\pi n_0 c_\beta \int_{r_i}^{r_j} r^2 g_{\alpha\beta}(r)\,\mathrm{d}r. \tag{4}$$

The functions $S_{NN}(Q)$ and $g_{NN}(r)$ are given directly by equations (1) and (2) if the scattering lengths of the atomic species are equal. Since $c_{Ge}\bar{n}_{Ge}^{Se} = c_{Se}\bar{n}_{Se}^{Ge}$ it then follows that the average coordination number, irrespective of the species type, is given by

$$\bar{n} = 4\pi n_0 \int_{r_i}^{r_j} r^2 g_{NN}(r)\,\mathrm{d}r = c_{Ge}(\bar{n}_{Ge}^{Ge} + \bar{n}_{Ge}^{Se}) + c_{Se}(\bar{n}_{Se}^{Se} + \bar{n}_{Se}^{Ge}). \tag{5}$$

For a binary Ge–Se system comprising elements of natural isotopic abundance the neutron scattering lengths are comparable at $b_{Ge} = 8.185(20)$ fm and $b_{Se} = 7.970(9)$ fm (Sears 1992). In the case of $GeSe_2$ the weighting coefficients are then calculated to be $A = 1.6(3) \times 10^{-4}$ and $B = 0.054(5)$ such that $S_{NN}(Q)$ accounts for 95% of $S_T(Q)$ i.e. the contribution from the other partial structure factors can, to first order, be neglected.

3. Experiment

Glassy $GeSe_2$ samples were prepared by loading Ge (99.9999%, Aldrich) and Se (99.999%, Johnson Matthey) into silica ampoules of 5 mm internal diameter and 1 mm wall thickness in a high purity argon filled glove box ($\approx$1 ppm oxygen, $<$10 ppm water). The ampoules had been cleaned using chromic acid prior to etching with a 40% solution of hydrofluoric acid. The sample-filled ampoules were then evacuated to a pressure of $\approx 10^{-5}$ Torr, purged three times

with helium gas and after ≈48 h they were sealed. Next, the ampoules were loaded into a rocking furnace, slowly heated at 1 °C min^{-1} to 1000 °C where they were left for 48 h, slowly cooled to 850 °C and finally quenched in an ice/salt-water mixture at ≈ −5 °C. The resultant $GeSe_2$ glass was then transferred to a cylindrical silica tube of 7 mm internal diameter and 1 mm wall thickness and sealed at room temperature under argon gas (99.998%) at a pressure of 0.41 atm ready for the diffraction experiment.

The neutron diffraction experiment was performed using the LAD instrument at the ISIS pulsed neutron source, Rutherford Appleton Laboratory. The complete experiment comprised the measurement of the diffraction patterns for the sample in its container in a cylindrical vanadium furnace, the empty container in the furnace, the empty furnace and a vanadium rod of 8.31(4) mm diameter in the furnace for normalization purposes. A thin vanadium sheath was used to conserve the shape of the silica cells at high temperatures. The data analysis was made using the ATLAS suite of programs (Soper *et al* 1989) and the nuclear cross-sections were taken from Sears (1992). The sample was measured at temperatures of 800(3), 1000(3) and 1100(3) °C where the number densities are 0.0312(2), 0.0317(2) and 0.0322(2) $Å^{-3}$ (Ruska and Thurn 1976) respectively. The corresponding argon gas over-pressure was estimated to be 1.56 atm, 1.82 atm and 1.94 atm respectively, assuming a negligible solubility of argon in the liquid. The melting point of $GeSe_2$ is at 742(2) °C (Ipser *et al* 1982).

LAD comprises 14 groups of detectors at scattering angles of ±5, ±10, ±20, ±35, ±60, ±90 and ±150° corresponding to instrumental resolution functions ($\Delta Q/Q$) of 11%, 6%, 2.8%, 1.7%, 1.2%, 0.8% and 0.5% respectively. The final $S_T(Q)$ functions were constructed by merging all those diffraction patterns from the different groups that showed good agreement. It was checked that the resultant functions $S_T(Q)$ tend to the correct high-Q limit, obey the usual sum rule relation and that there is good overall agreement between each $S_T(Q)$ and the back-Fourier transform of the corresponding $G_T(r)$ after the unphysical low-r oscillations are set to their calculated $G_T(0)$ limit (Salmon and Benmore 1992).

4. Results

The measured $S_{NN}(Q)$, as obtained from equation (1) by assuming $A = B = 0$, are shown in figure 1. As the temperature is increased the height of the FSDP decreases markedly and its position Q_1 moves from 0.99(1) to 1.05(1) $Å^{-1}$ via 1.02(1) $Å^{-1}$. At the same time its full-width at half-maximum ΔQ_1, as measured on making the peak symmetrical by reflecting its low-Q part about Q_1, increases from 0.43(1) to 0.51(1) $Å^{-1}$ via 0.50(1) $Å^{-1}$. Furthermore, the third peak becomes smaller relative to the second and the high-Q oscillations become increasingly damped, consistent with a broadening of the distribution of nearest neighbours in real space. Similar trends with increasing temperature have also been observed for liquid As_2Se_3 from

Table 1. Parameters describing $S_{NN}(Q)$ for molten $GeSe_2$ and GeSe where Q_ε ($\varepsilon = 1, 2, 3, 4$) gives the position of peak ε. The data for $GeSe_2$ at 784 °C and GeSe at 727 °C are taken from Penfold and Salmon (1991) and Petri *et al* (1999a) respectively.

System	T(°C)	Q_2 ($Å^{-1}$)	Q_1/Q_2	Q_3/Q_2	Q_4/Q_2	$S_{NN}(Q_2)$	$S_{NN}(Q_1)/S_{NN}(Q_2)$	$S_{NN}(Q_3)/S_{NN}(Q_2)$	$S_{NN}(Q_4)/S_{NN}(Q_2)$
$GeSe_2$	784(3)	2.02(2)	0.49	1.75	2.80	1.14(1)	0.67	1.24	1.00
	800(3)	2.03(1)	0.49	1.73	2.81	1.10(1)	0.63	1.24	1.03
	1000(3)	2.13(1)	0.48	1.64	2.66	1.07(1)	0.47	1.18	1.04
	1100(3)	2.22(1)	0.47	1.57	2.58	1.10(1)	0.38	1.09	0.99
GeSe	727(2)	2.23(1)	0.53	1.57	2.51	1.32(1)	0.19	0.98	0.86

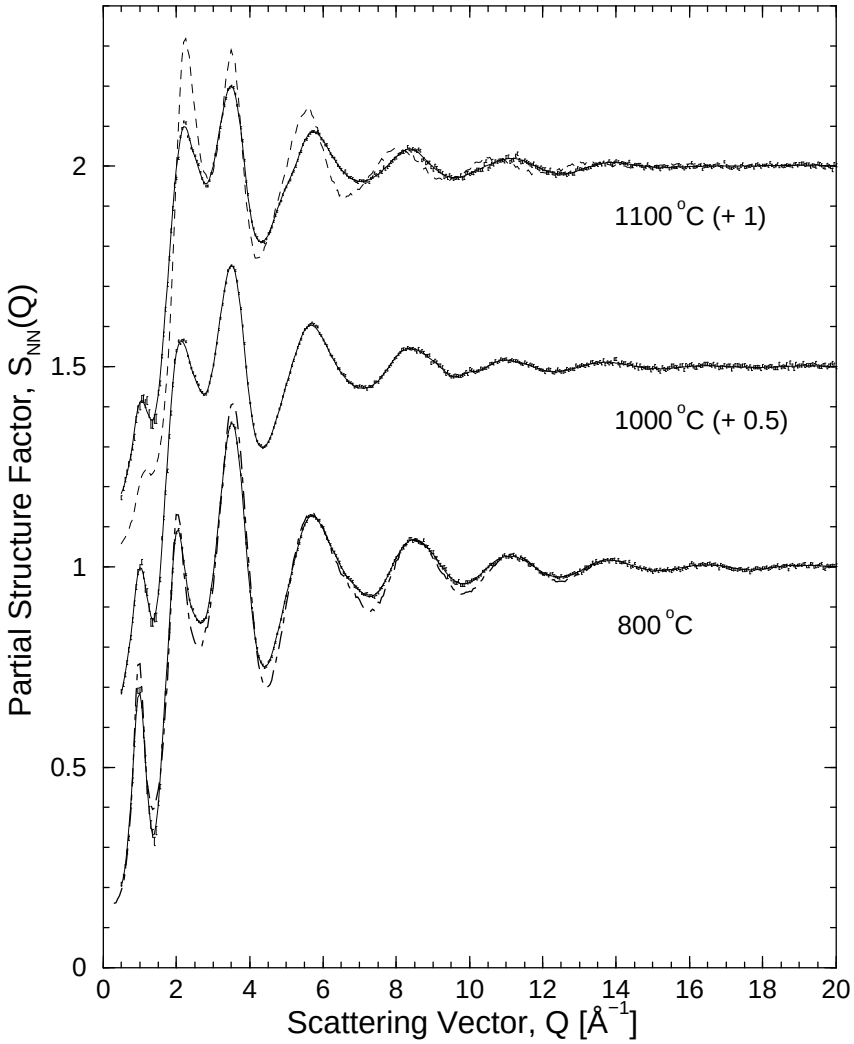

Figure 1. The measured $S_{NN}(Q) = S_T(Q) + 1$ for liquid $GeSe_2$ at 800, 1000 and 1100 °C as obtained from equation (1) by assuming $A = B = 0$. The bars represent the statistical errors on the data points and the solid curves are the smoothed $S_{NN}(Q)$ obtained by using a cubic spline fit to those data points. The chained curve superimposed on the lower data set gives $S_{NN}(Q)$ for molten $GeSe_2$ at 784 °C (Penfold and Salmon 1991) and the dashed curve superimposed on the upper data set gives $S_{NN}(Q)$ for molten GeSe at 727 °C (Petri *et al* 1999a).

x-ray diffraction experiments (Hosokawa *et al* 1992). A summary of the parameters describing the $S_{NN}(Q)$ functions for molten $GeSe_2$ is given in table 1.

The corresponding $g_{NN}(r)$ are shown in figure 2 and the parameters describing the first and second nearest neighbours are given in table 2. The r_1 and $\bar{n}$ values are in accord with those measured for $GeSe_2$ in the temperature range from 800 to 900 °C by Maruyama *et al* (1996). It is found that although there is a notable broadening of the first two peaks with increasing temperature, neither their position nor the average coordination number $\bar{n}$ change within the experimental error.

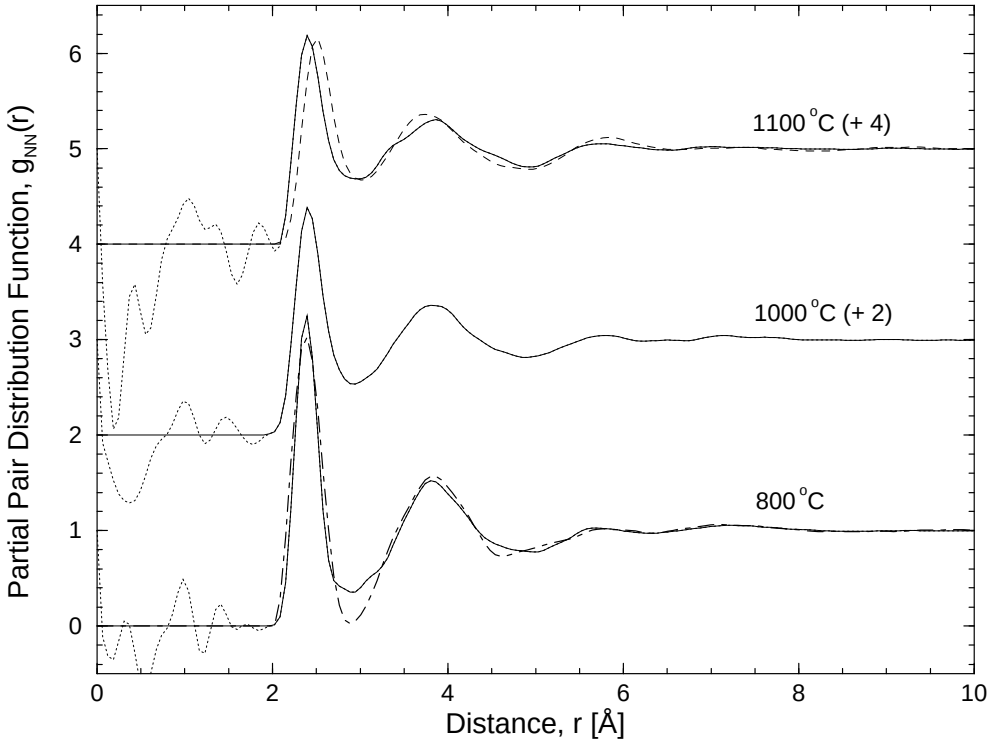

Figure 2. The measured $g_{NN}(r)$ for liquid $GeSe_2$ at 800, 1000 and 1100 °C as obtained by Fourier transforming the smoothed $S_{NN}(Q)$ given by the solid curves in figure 1. The unphysical low-r oscillations about the $g_{NN}(0)$ limits are shown by the broken curves. The chained curve superimposed on the lower data set gives $g_{NN}(r)$ for molten $GeSe_2$ at 784 °C (Penfold and Salmon 1991) and the dashed curve superimposed on the upper data set gives $g_{NN}(r)$ for molten GeSe at 727 °C (Petri *et al* 1999a).

Table 2. Interatomic distances and coordination numbers for molten $GeSe_2$ and GeSe where r_1 and r_2 give the positions of the first and second peaks in $g_{NN}(r)$. The data for $GeSe_2$ at 784 °C and GeSe at 727 °C are taken from Penfold and Salmon (1991) and Petri *et al* (1999a) respectively.

System	T(°C)	r_1 (Å)	r_2/r_1	$\bar{n}$	Integration range (Å)
$GeSe_2$	784(3)	2.38(2)	1.609	2.8(1)	2.02(1)–2.95(1)
	800(3)	2.38(2)	1.605	2.7(1)	1.90(1)–2.95(2)
	1000(3)	2.40(2)	1.596	2.7(1)	1.90(1)–3.01(2)
	1100(3)	2.40(2)	1.608	2.6(1)	2.09(1)–3.01(2)
GeSe	727(2)	2.52(2)	1.452	3.5(3)	2.09(2)–3.04(2)

5. Discussion

The $S_{NN}(Q)$ function measured by a full partial structure factor analysis of liquid $GeSe_2$ at 784(3) °C (Penfold and Salmon 1991, Salmon 1992) is compared in figure 1 with that at 800 °C derived from the present work. The overall profiles of the functions are comparable, the sharper peaks at 784 °C corresponding to a lower liquid temperature. The limitations of the approximation $A = B = 0$ in equation (1) can be seen in figure 2 where $g_{NN}(r)$ at 784 °C is compared with the approximate $g_{NN}(r)$ at 800 °C. The latter is found to be higher

in the regions around the first peak at 2.38(2) Å and the first minimum at 2.95(2) Å and lower in the region around the second peak at 3.82(2) Å. These discrepancies can be ascribed to the finite value of B in equation (2) which gives an additional contribution to $G_T(r)$from $g_{NC}(r)$ and hence, through equation (3*c*), additional positive contributions from $g_{GeSe}(r)$ and $g_{GeGe}(r)$ and negative contributions from $g_{SeSe}(r)$. The discrepancies in figure 2 can thereby be rationalized since the strongest real-space features are the first main peaks in $g_{GeSe}(r)$, $g_{GeGe}(r)$ and $g_{SeSe}(r)$ at 2.42(2), ≈3.3 and 3.80(2) Å respectively (Penfold and Salmon 1991). Notwithstanding, there is a good overall level of agreement between the measured and estimated $g_{NN}(r)$ functions which demonstrates that the approximation $A = B = 0$ is good to first order.

If it is assumed that the first peak in each of the $G_T(r)$ functions comprises Ge–Se correlations alone, then mean coordination numbers $\bar{n}_{Ge}^{Se}$ of 3.9(1), 4.0(2) and 3.9(2) are obtained for 800, 1000 and 1100 °C respectively. These coordination numbers indicate that $Ge(Se_{1/2})_4$ tetrahedra remain the dominant structural motifs at all three temperatures. They are, however, larger than the value $\bar{n}_{Ge}^{Se} = 3.6(3)$ obtained from the measured $g_{GeSe}(r)$ for liquid $GeSe_2$ at 784 °C, which is consistent with the presence of homopolar bonds (Penfold and Salmon 1991). There is no evidence for an increase in the coordination number from four to six with increasing temperature and density, in contrast to earlier deductions based on several of the physico-chemical properties of $GeSe_2$ (Ruska and Thurn 1976).

Rather, the density increase with temperature results from a breakdown of the intermediate range atomic ordering of the network melt as manifest by the changes in the FSDP. This feature has a dominant contribution from the Ge–Ge correlations (Penfold and Salmon 1991) and the shift of its position to higher Q-values implies a reduction in the periodicity $2\pi/Q_1$ of the corresponding density fluctuations. The decrease in its height implies a reduction in the magnitude of these fluctuations and the increase in its width implies a diminution in the coherence length from $2\pi/\Delta Q_1 = 14.6(3)$ Å at 800 °C to 12.4(3) Å at 1100 °C (Salmon 1994). Thus, although the changes in height and position of the FSDP are comparatively small between the glass at low temperature and the liquid above its melting point (Susman *et al* 1988, 1990), substantial changes are clearly apparent as the liquid temperature is raised.

The observed trend in the shapes of $S_{NN}(Q)$ and $g_{NN}(r)$ for liquid $GeSe_2$ with increasing temperature strongly mimics that observed in the liquid phase as germanium is added to $GeSe_2$ to form GeSe (Salmon and Liu 1994). For example, the FSDP disappears with increasing germanium content, the second peak in $S_{NN}(Q)$ becomes comparable in height to the third peak and the first peak in $g_{NN}(r)$ undergoes a strong reduction in height. To help illustrate this point, the measured $S_{NN}(Q)$ and $g_{NN}(r)$ functions for liquid GeSe at 727(2) °C (Petri *et al* 1999a) are compared with those for $GeSe_2$ at 1100 °C in figures 1 and 2 respectively. The similarity is not, however, anticipated to result from a significant loss of selenium from the melt in the present work. For example, by considering the $GeSe_2$ sample at 1100 °C to be a system of two non-interacting liquids in equilibrium with Se_2 dimers in the gas phase, a ratio of 1 Ge:1.95 Se is estimated for the melt by using the vapour pressures for pure Ge and Se (Weast 1986). The actual stoichiometry is anticipated to be closer to 1 Ge:2 Se owing to the Ge–Se bonding and the use of an argon gas over-pressure.

A structural similarity between liquid $GeSe_2$ at high temperature and liquid GeSe at a somewhat lower temperature might be anticipated on the basis of several of the physico-chemical properties of these materials. For example, the electrical conductivity is 60 Ω^{-1} cm^{-1} for $GeSe_2$ at ≈1040 °C and GeSe at ≈700 °C, the thermopower is 100 μV K^{-1} for $GeSe_2$ at ≈1020 °C and GeSe at ≈700 °C, and the conductivity gap is zero for $GeSe_2$ at 1073 °C and GeSe at 750 °C (Okada *et al* 1996). Also, the viscosity of $GeSe_2$ rapidly becomes comparable to that

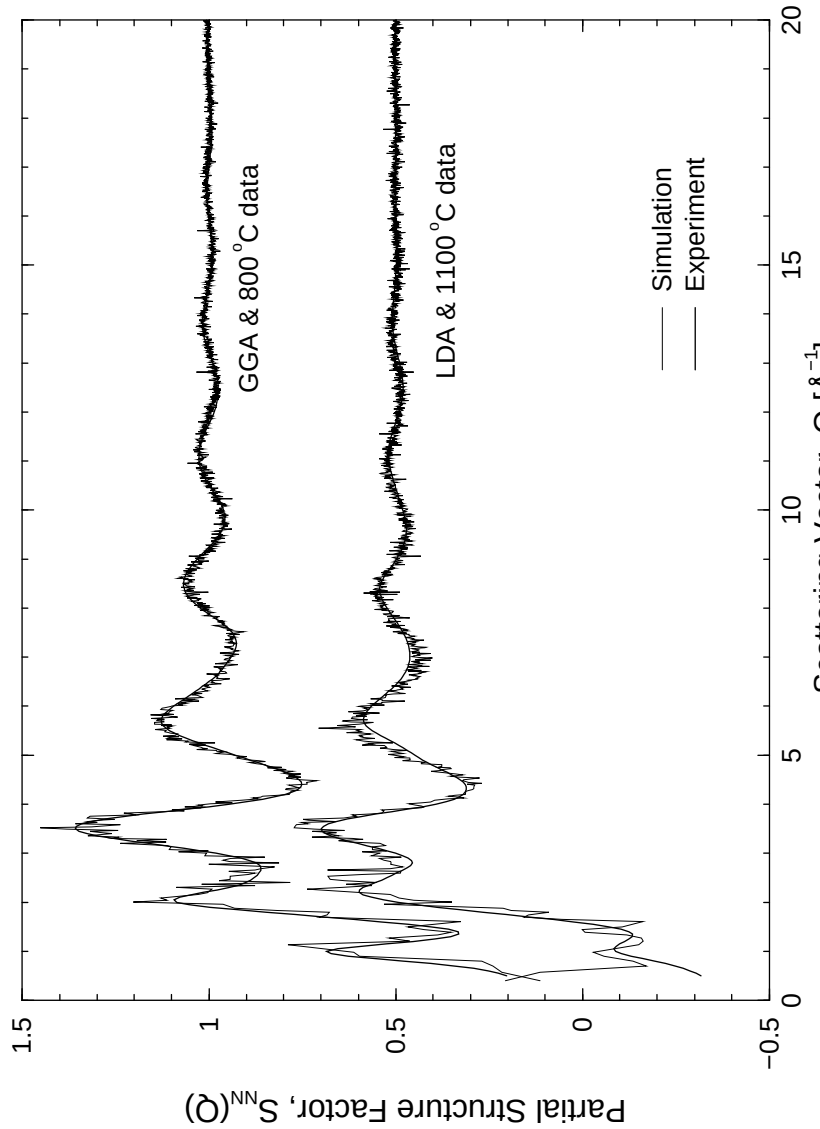

Figure 3. The measured $S_{NN}(Q)$ for liquid $GeSe_2$ at 800 °C and 1100 °C given in figure 1 compared with the *ab initio* molecular dynamics results for liquid $GeSe_2$ at ~747 °C calculated by using the GGA and LDA schemes respectively (Massobrio *et al* 1999). The bold solid curves give the experimental data and the fine solid curves the simulated structures. The lower two curves have been shifted vertically by −0.5.

for GeSe with rising temperature (Glazov and Situlina 1969). Although the profiles of $g_{NN}(r)$ for liquid GeSe at 727 °C and liquid $GeSe_2$ at 1100 °C are similar (figure 2), the structures are not, however, identical, as shown, for example, by the nearest-neighbour distance which is 5% larger at 2.52(2) Å in liquid GeSe. Nevertheless, it would be interesting to perform diffraction experiments on $GeSe_2$ at higher temperatures through the semiconductor to metal transition to see if $S_{NN}(Q)$ begins to resemble the structure factor for metallic liquid germanium (Salmon and Liu 1994).

In a recent Car–Parinello type *ab initio* molecular dynamics study of liquid $GeSe_2$ at ∼747 °C the results obtained by treating the electronic structure using two different approximations within density functional theory, namely the local density approximation (LDA) and the generalized gradient approximation (GGA), were considered (Massobrio *et al* 1999). It was found that when compared with the LDA scheme, the GGA scheme gives rise to an increase in the ionic character of the bonding. This leads to a reduction in the number of homopolar bonds and the concomitant enhancement in the chemical ordering results in the formation of more $Ge(Se_{1/2})_4$ tetrahedral units, which in turn leads to the establishment of intermediate range atomic ordering as manifest by the appearance of an FSDP. Use of the GGA functional was required to obtain best agreement with the structure measured for liquid $GeSe_2$ at 784 °C (figure 3) and it was concluded that this scheme is crucial for describing the structural ordering in disordered covalent systems (Massobrio *et al* 1998, 1999). Notably, the structure calculated for $GeSe_2$ at ∼747 °C using the LDA scheme bears a strong resemblance to that measured for liquid $GeSe_2$ at the higher temperature of 1100 °C (figure 3) in addition to that measured for liquid GeSe at 727 °C (Petri *et al* 1999a, b). It would therefore be interesting to investigate the sensitivity to both temperature and concentration of the structures simulated by using both the LDA and GGA schemes as it would appear that the Ge–Se binary system offers a sensitive test-bed for the methods used in current *ab initio* molecular dynamics simulations.

Finally, liquid GeSe at 727 °C has a substantial number of homopolar bonds. Each Ge has an average of 0.8(1) Ge at 2.36(2) Å and 3.2(2) Se at 2.54(2) Å while each Se has 0.22(3) nearest-neighbouring Se at 2.34(2) Å (Petri *et al* 1999a, b). Further, the structure of $GeSe_2$ simulated using the LDA has more homopolar bonds than that calculated using the GGA. The similarity between the total structure factor measured for $GeSe_2$ at 1100 °C and those measured for GeSe and calculated for $GeSe_2$ using the LDA may therefore indicate that the number of homopolar bonds in liquid $GeSe_2$ increases with temperature. Such an increase has already been observed in liquid As_2Se_3 (Tamura *et al* 1992, Shimojo *et al* 1999). The detailed structure of bulk quenched $GeSe_2$ and As_2Se_3 glasses should therefore depend on the temperature from which the melt is quenched in addition to the quench rate.

6. Conclusions

As the temperature of liquid $GeSe_2$ is raised above its melting point to 1100 °C, there is a broadening in the distribution of nearest neighbours but their mean position and coordination number $\bar{n}$ do not change at the level of $g_{NN}(r)$. Instead, the accompanying increase in density and decrease in viscosity result from a destruction of the intermediate range atomic ordering associated with the Ge–Ge correlations as manifest by the reduction in intensity of the FSDP and its shift in position to higher Q-values. The changes in the profiles of $S_{NN}(Q)$ and $g_{NN}(r)$ for liquid $GeSe_2$ with increasing temperature mimic those observed as the composition of liquid $GeSe_2$ is altered to the GeSe stoichiometry by the addition of germanium. The results suggest that the binary Ge–Se system will offer further challenges to the methods used in current Car–Parinello type *ab initio* molecular dynamics simulations.

Acknowledgments

It is a pleasure to thank Chris Goodway for help with the LAD furnace, Carlo Massobrio and Alfredo Pasquarello for useful discussions, Tatsuya Okada for the electrical conductivity data and the EPSRC for support. IP also thanks the University of East Anglia for financial assistance and PSS thanks the British Council for making possible helpful discussions with the Liquids Group in Hiroshima.

References

Andreev A A, Melekh B T and Turgunov T 1976 *Sov. Phys.–Solid State* **18** 141
Bhatia A B and Thornton D E 1970 *Phys. Rev.* B **2** 3004
Fischer-Colbrie A and Fuoss P H 1990 *J. Non-Cryst. Solids* **126** 1
Glazov V M and Situlina O V 1969 *Doklady Chemistry* **187** 587
Hosokawa S, Sakaguchi Y, Hiasa H and Tamura K 1991 *J. Phys.: Condens. Matter* **3** 6673
Hosokawa S, Sakaguchi Y and Tamura K 1992 *J. Non-Cryst. Solids* **150** 35
Ipser H, Gambino M and Schuster W 1982 *Monat. Chem.* **113** 389
Laugier A, Chaussemy G and Fornazero J 1977 *J. Non-Cryst. Solids* **23** 419
Maruyama K, Misawa M, Inui M, Takeda S, Kawakita Y and Tamaki S 1996 *J. Non-Cryst. Solids* **205–207** 106
Massobrio C, Pasquarello A and Car R 1998 *Phys. Rev. Lett.* **80** 2342
——1999 *J. Am. Chem. Soc.* **121** 2943
Okada T, Satoh T, Matsumura M and Ohno S 1996 *J. Phys. Soc. Japan* **65** 230
Penfold I T and Salmon P S 1991 *Phys. Rev. Lett.* **67** 97
——1992 *Phys. Rev. Lett.* **68** 253
Petri I, Salmon P S and Fischer H E 1999a *J. Phys.: Condens. Matter* **11** 7051
——1999b *J. Non-Cryst. Solids* **250–252** 405
Ruska J and Thurn H 1976 *J. Non-Cryst. Solids* **22** 277
Salmon P S 1992 *Proc. R. Soc.* A **437** 591
——1994 *Proc. R. Soc.* A **445** 351
Salmon P S and Benmore C J 1992 *Recent Developments in the Physics of Fluids* ed W S Howells and A K Soper (Bristol: Hilger) p F225
Salmon P S and Liu J 1994 *J. Phys.: Condens. Matter* **6** 1449
Sears V F 1992 *Neutron News* **3** 26
Shimojo F, Munejiri S, Hoshino K and Zempo Y 1999 *J. Phys.: Condens. Matter* **11** L153
Soper A K, Howells W S and Hannon A C 1989 *Rutherford Appleton Laboratory Report* RAL-89-046
Susman S, Price D L, Volin K J, Dejus R J and Montague D G 1988 *J. Non-Cryst. Solids* **106** 26
Susman S, Volin K J, Montague D G and Price D L 1990 *J. Non-Cryst. Solids* **125** 168
Tamura K, Hosokawa S, Inui M, Yao M, Endo H and Hoshino H 1992 *J. Non-Cryst. Solids* **150** 351
Weast R C (ed) 1986 *CRC Handbook of Chemistry and Physics* 67th edn (Boca Raton, FL: Chemical Rubber Company)
Wright A C, Sinclair R N and Leadbetter A J 1985 *J. Non-Cryst. Solids* **71** 295